JOURNAL OF GEOPHYSICAL RESEARCH, VOL. 112, C12023, doi:10.1029/2007JC004222, 2007

Water mass characteristics in the equatorial North Atlantic: A section nominally along 6.5°N, July 2000

Artem Sarafanov,[1] Alexey Sokov,[1] and Alexander Demidov[2]

Received 20 March 2007; revised 15 August 2007; accepted 14 September 2007; published 29 December 2007.

[1] In July 2000, a transatlantic conductivity-temperature-depth/hydrographic section was occupied on board the Russian R/V *Akademik Ioffe* in the northern equatorial region from 9°26′N, 17°22′W to 3°48′N, 47°16′W near the World Ocean Circulation Experiment (WOCE) A06 line. The water mass characteristics and the main features of cross-sectional circulation are reported on the basis of the potential temperature, salinity, potential density, and silicate distributions along the section. A scheme of the upper ocean circulation dominated by the near-surface eastward North Equatorial Countercurrent, most intense at 5.5°–6°N, and the subsurface cyclonic flow of the North Equatorial Undercurrent, is presented. The boundary flows along the Brazilian slope are revealed at the Upper and Lower North Atlantic Deep Water (NADW) levels, while the main pathways of intermediate waters and the Middle NADW are offshore. The northward recirculation of NADW is observed in both the western and eastern basins; in particular, a reversal of the Deep Western Boundary Current at the Middle NADW level is detected. The warming of the intermediate, deep, and near-bottom waters in the interior eastern basin is revealed from comparison of the section temperature data with those obtained at the WOCE A06 line in 1993. The substantial 1993–2000 temperature increase (+0.02°C–0.1°C) at the intermediate and upper deep levels suggests that the previously reported long-term warming above 2500–3000 m in the equatorial and subtropical North Atlantic between the late 1950s and early 1990s continued in the interior eastern equatorial basin during the last decade of the 20th century.

Citation: Sarafanov, A., A. Sokov, and A. Demidov (2007), Water mass characteristics in the equatorial North Atlantic: A section nominally along 6.5°N, July 2000, *J. Geophys. Res.*, *112*, C12023, doi:10.1029/2007JC004222.

1. Introduction

[2] The global oceanic conveyor belt [*Broecker*, 1985] transports the cold North Atlantic Deep Water formed by convection and mixing in the northern North Atlantic southward [e.g., *Dickson and Brown*, 1994]. The compensating return flow at shallow levels carries warmer water from the Pacific and Indian Oceans to the North Atlantic [e.g., *Gordon*, 1986; *Rintoul*, 1991]. Subpolar and polar waters, namely, the Antarctic Intermediate Water, Upper Circumpolar Water and Antarctic Bottom Water, move across the equator from the South Atlantic mainly in the western basin (*Arhan et al.* [1998] (hereinafter referred to as A98) and *Oudot et al.* [1999]) and contribute to the interocean overturning cell [*Schmitz*, 1995; *Macdonald*, 1998]. The equatorial Atlantic, being thus a key transit region for the global circulation is the area of increased oceanographic interest.

[3] The first basin-wide zonal section in the northern equatorial Atlantic was carried out along 8.25°N during the cruise 10 of R/V *Crawford* in May 1957 within the framework of the International Geophysical Year [*Fuglister*, 1960]. The most detailed recent studies [*Andrie et al.*, 1998; A98; *Oudot et al.*, 1998, 1999] to which we first of all refer are based on the data obtained during the CITHER-1 cruise on board the French R/V *L'Atalante* in 1993. Analysis of distributions of hydrographic properties and nutrients along 7.5°N and 4.5°S zonal sections (World Ocean Circulation Experiment (WOCE) A06 and A07 lines) and two meridional ones along 4°W and 35°W has provided a complex description of the Atlantic water masses at their crossing the equator. Since 1993, no basin-wide zonal sections (except for the section presented herein) were carried out in the region in question.

[4] In July 2000, the hydrographic section nominally along a latitude of 6.5°N (see Figure 1) was occupied during the cruise 8 of the Russian R/V *Akademik Ioffe*. Cruise was carried out within the framework of the "World Ocean" Russian Federal Program in order to investigate the interaction processes between the North and South Atlantic and to supplement the global baseline data for the study of the interocean circulation. This paper is based mainly on the original conductivity-temperature-depth (CTD) and silicate data from the section (hereinafter referred to as the Ioffe-2000 section). We provide a brief presentation of the data (section 2), describe the upper ocean cross-sectional circu-

[1]P. P. Shirshov Institute of Oceanology, Moscow, Russia.
[2]Department of Oceanology, Moscow State University, Moscow, Russia.

0148-0227/07/2007JC004222$09.00

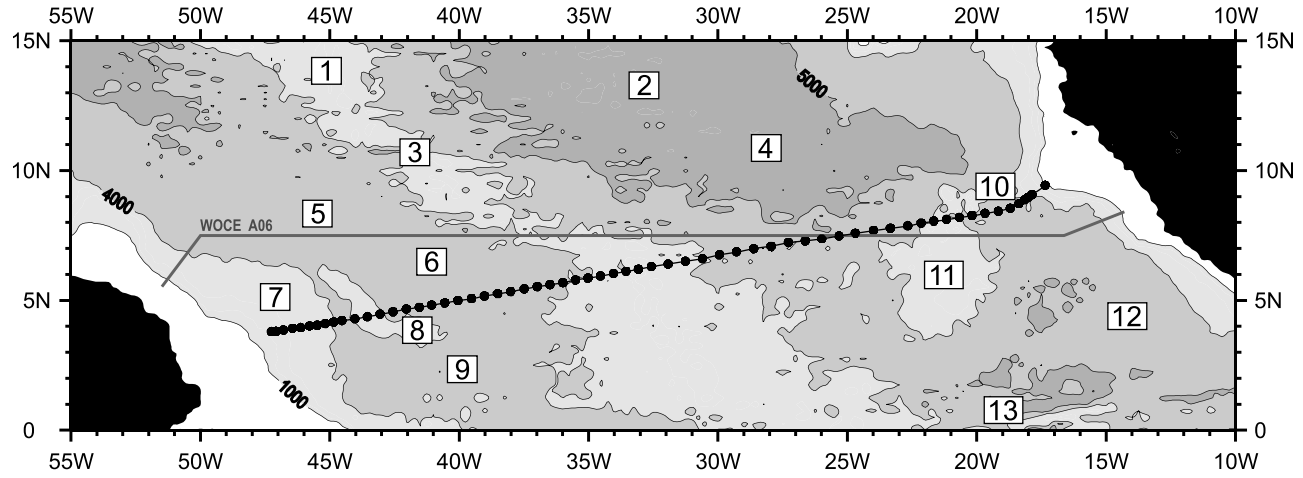

Figure 1. Station locations of the section occupied on the R/V *Akademik Ioffe*, 13–28 July 2000. The WOCE A06 line (7.5°N) is shown. Numbers within rectangles show the typical topographic sites: 1, Mid-Atlantic Ridge; 2, Cape Verde Basin; 3, Vema Fracture Zone; 4, Gambia Abyssal Plain; 5, Guiana Basin; 6, Para Abyssal Plain; 7, Amazon Cone; 8, Ceara Rise; 9, Ceara Abyssal Plain; 10, Kane Gap; 11, Sierra Leone Rise; 12, Sierra Leone Basin; 13, Romanche Fracture Zone.

lation (section 3), and report the observed water mass properties, the main circulation features at the intermediate and deeper levels (section 4) and the temperature changes between the 1993 and 2000 observations (section 5). In the absence of data from direct current measurements (not performed in the cruise), the cross-sectional circulation is inferred from the potential density distribution. Thus the derived circulation features do not take into account an unmeasured barotropic component, which could alter the results to some extent.

[5] The 1993–2000 temperature changes are discussed in the context of the previously reported apparent long-term warming above ~3000 m and cooling of the deeper waters in the equatorial and subtropical North Atlantic between the late 1950s and early 1990s [*Parrilla et al.*, 1994; A98].

[6] Being close to the WOCE A06 line, the Ioffe-2000 section does not repeat the former. The reason for this was a limited cruise duration, which forced us to choose the shorter track. As a result, the section line is rotated counterclockwise from the A06 line, intersecting the latter in the central part of the eastern basin at 25°W (Figure 1). The western end of the section is located ~400 km south of the A06 line, and the easternmost station was carried out ~200 km north of A06. This difference in the section locations is certainly crucial to the quantitative comparison of the entire Ioffe-2000 section with the 1993 occupation of A06 (CITHER-1 7.5°N section). Nevertheless, in order to reveal a possible 7-year (a) changes in the eastern basin, comparison of the temperature data from the 1993 and 2000 sections is carried out for their 22–28°W intersecting segments, meridional distance between the ends of which does not exceed 50 km.

2. Data and Bathymetry

[7] A long CTD/hydrographic transect with closely spaced 62 stations was occupied on 13–28 July 2000 along the nominal longitude of 6.5°N between the continental slopes of Guinea and Brazil (Figure 1). The section line starts at the point (9°26′N, 17°22′W), the depth of 985 m, intersects the northern edge of the Sierra Leone Basin near the Kane Gap (18°–21°W), the northern shoulder of the Sierra Leone Rise (21°–22°W), then runs along the southern boundary of the Gambia Abyssal Plain and crosses the MAR at 31–36°W. In the western basin, the section line goes through the Guiana Basin, where it intersects the Para Abyssal Plain (36°–43°W), the Ceara Rise, the northwestern periphery of the Ceara Abyssal Plain at ~45°W, the Amazon Cone and reaches its final point (3°48′N, 47°16′W), the depth of 2298 m. Because of border clearance issues, the work was stopped ~100 km from the Brazilian shelf. The nominal station spacing of ~55 km was increased up to ~75 km over abyssal plain in the eastern basin and reduced to ~25–35 km over the continental slopes.

[8] The temperature and salinity data were obtained with an oceanographic Neil Brown Mark-III CTD profiler. At all stations, water samples for salinity and silicate concentrations were obtained at 8–12 depths from ~50 m to 3000–3200 m. The silicate concentrations were determined according to the standard method [*Mullin and Riley*, 1955]. The accuracy of measurements was 0.002°C for temperature, 0.002 psu for salinity and better than 0.2 μmol mol kg^{-1} for silicate. The temperature accuracy was determined via precruise and postcruise laboratory calibrations, and the salinity accuracy was calculated by comparison with the bottle data. The temperature data accuracy and the station spacing of the Ioffe-2000 section are practically the same as those of the CITHER-1 7.5°N section (see A98), the data from which we use for the 1993–2000 temperature comparison in section 5.

[9] Vertical distributions of potential temperature (θ), salinity (S), potential density ($\sigma_0/\sigma_2/\sigma_4$) and silicate (Si) along the section are displayed in Figure 2; the expanded view of the potential density distribution above 1000 m is shown in Figure 3a. The θ-S and θ-Si diagrams for the data

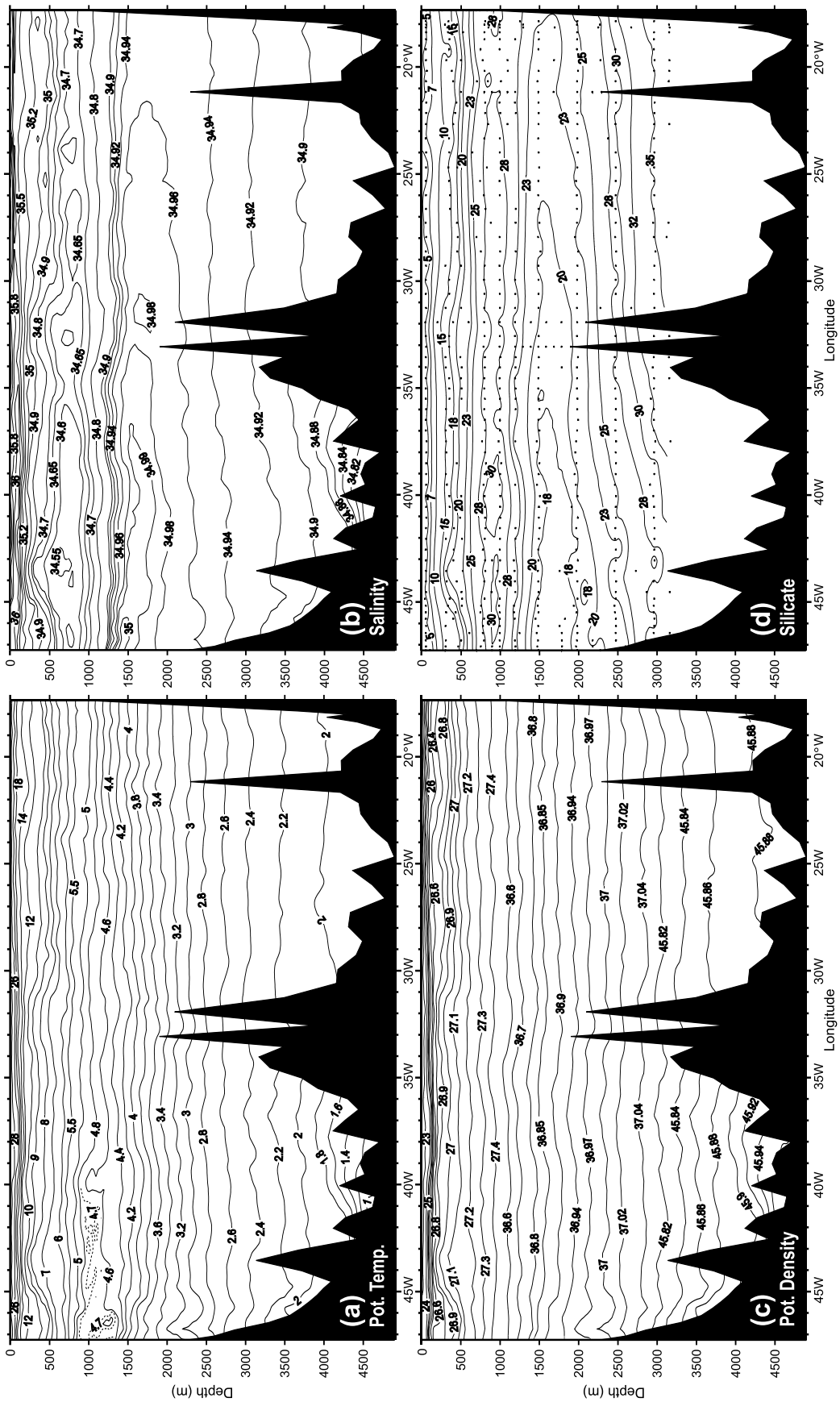

Figure 2. Vertical distributions of (a) potential temperature (°C), (b) salinity, (c) potential density ($\sigma_0/\sigma_2/\sigma_4$, kg m^{-3}), and (d) silicate (μmol kg^{-1}) along the Ioffe-2000 section. Dashed isotherm 4.7°C in Figure 2a marks the temperature minimum layer. Dots in Figure 2d show the bottle locations.

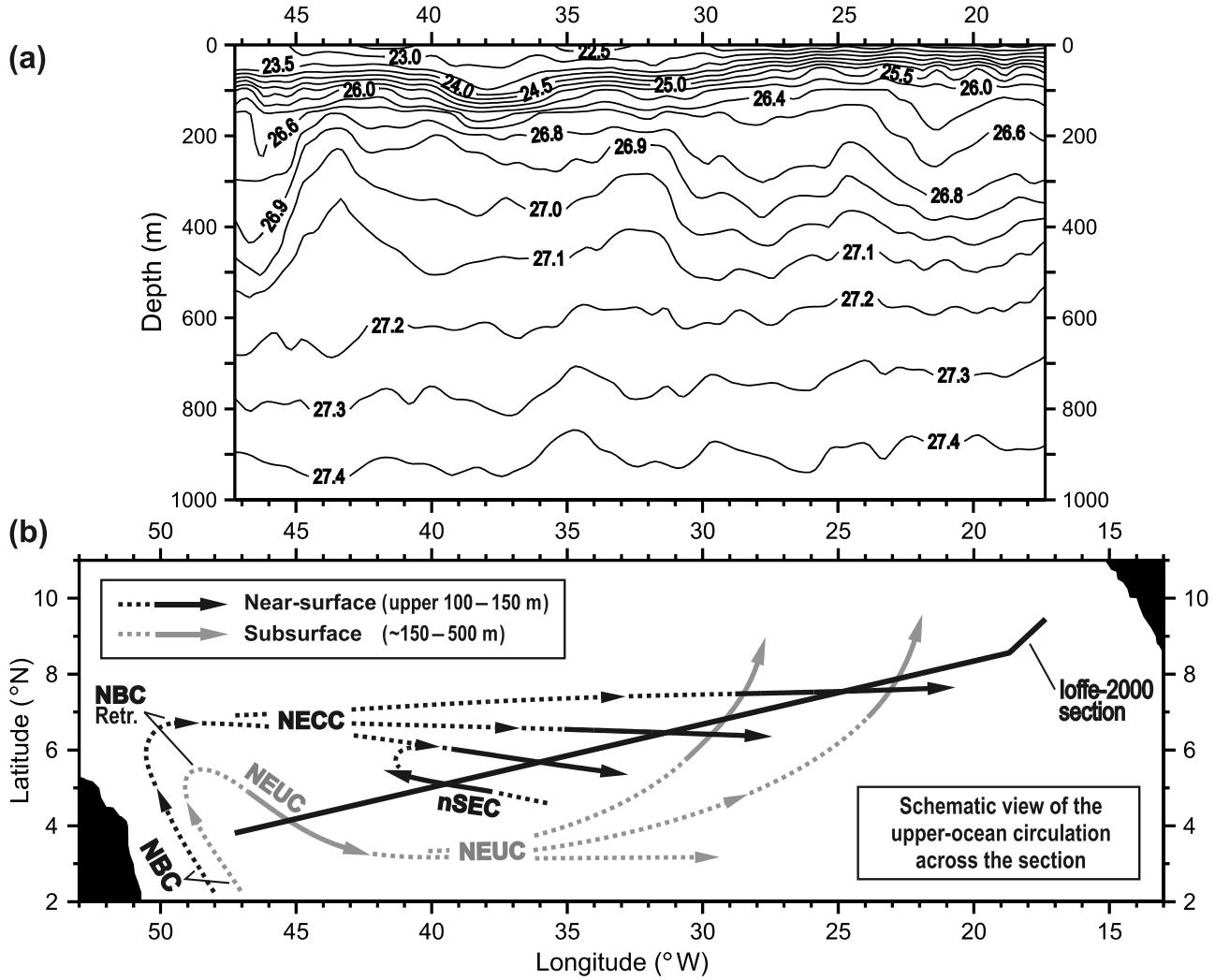

Figure 3. On the description of the upper ocean circulation. (a) Expanded view of the potential density (σ_0, kg m^{-3}) vertical distribution along the Ioffe-2000 section within the upper 1000 m layer. (b) Schematic representation of the near-surface (upper 100–150 m, $\sigma_0 < 26.0$ kg m^{-3}) and subsurface (~150–500 m, $26.0 < \sigma_0 < 27.0$ kg m^{-3}) circulation in the region crossed by the section, including the North Brazil Current (NBC) and its retroflection (NBC Retr.), the North Equatorial Countercurrent (NECC), northern branch of the South Equatorial Current (nSEC), and the North Equatorial Undercurrent (NEUC). The cross-sectional flows derived from the vertical distribution of potential density are sketched with solid arrows. Dashed arrows are used to schematically visualize the assumed off-sectional flows; see section 3 for details.

from measurements at intermediate and deeper levels are given in Figure 4.

3. Upper Ocean Circulation

[10] The warm (>9–10°C), high-saline (>34.9) and silicate-poor (<15 μmol kg^{-1}) waters observed in the section above 400–500 m, $\sigma_0 < 27.0$ kg m^{-3} (Figures 2 and 3a), are initially advected to the equatorial North Atlantic mostly by the North Brazil Current (NBC), flowing along the Brazilian coast from the southern equatorial region [e.g., *Schott et al.*, 1993; *Schmitz and McCartney*, 1993]. At the upper levels, above the pycnocline, the NBC carries the Salinity Maximum Water formed by evaporation in the tropics, and below the pycnocline (at depths of ~150–500 m), the current conveys the South Atlantic Central Water (SACW) thus contributing to the upper limb of the Atlantic meridional overturning cell [see A98; *Blanke et al.*, 2002; *Stramma et al.*, 2005a]. Having passed the equator, the NBC proceeds northwestward as a boundary flow, crossing a latitude of the Ioffe-2000 section western end (3.8°N) east of ~47°W [see *Johns et al.*, 1998]. Since the westernmost station of the section was carried out at 47°16′W, the boundary flow of the NBC is not seen from the Ioffe-2000 data. However, the general seaward deepening of the isopycnals at depths of ~150–500 m between 46°W and 47°W (Figure 3a) can be considered as a probable signature of the NBC eastern periphery.

[11] Further northwest (at 6°–7°N), the upper part of the NBC seasonally, in boreal summer–fall, retroflects into the

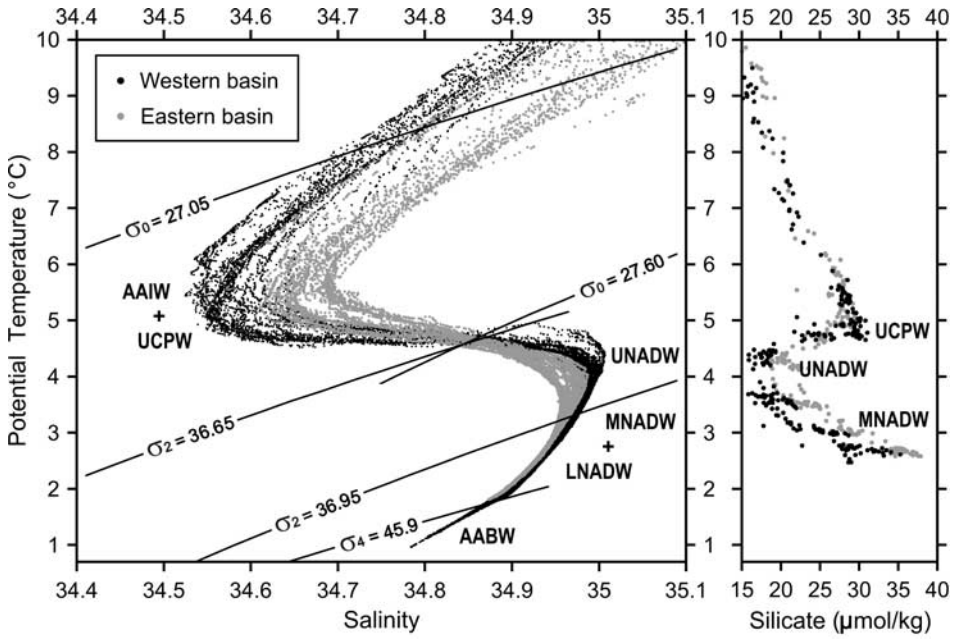

Figure 4. Plots of salinity and silicate (μmol kg^{-1}) versus potential temperature (°C) based on the Ioffe-2000 data. The data points from the western (west of 32.5°W) and eastern basins are indicated by black and gray dots, respectively. The isopycnals matching the approximate water mass limits are shown. See text for water mass abbreviations.

eastward North Equatorial Countercurrent (NECC). During the winter–spring, the retroflection subsides, the NBC proceeds toward the Caribbean Sea, and the NECC weakens and even reverses west of 20°W [*Richardson and McKee*, 1984; *Johns et al.*, 1998].

[12] Unlike the CITHER-1 7.5°N section, which was occupied in winter (13 February to 5 March 1993), the Ioffe-2000 transect was completed in the second half of July, when the NECC is expected to be well developed. The salinity distribution along the section depicts the eastward cross-sectional flow of the saline (~35.5–36.2) waters carried by NECC in the upper ~150-m layer. The current is evident in the potential density pattern from the eastward rise of the pycnocline isopycnals ($\sigma_0 \leq 26.0$ kg m^{-3}) between 38°W and 23°–25°W. Thus, taking into account the section orientation (see Figure 1), the NECC is detected within the 5.3°–7.8°N latitude belt. The most intense cross-sectional flow of the NECC is seen from the steep isopycnal slopes at 35°–37°W (~5.5°–6°N). This result agrees with the drifter observations of *Lumpkin and Garzoli* [2005, Figure 8], according to which the NECC at 30–40°W is centered between 5°N and 7°N.

[13] Immediately southwest of the NECC, at ~38°–41°W (~5°–5.5°N), the steep eastward deepening of pycnocline isopycnals indicates the northwestward or northward near-surface flow. The similar flow was previously revealed from the drifter observations and it was associated with the northern branch of the South Equatorial Current, which does not reach the Brazilian coast but instead recirculates northward into the NECC at around 5°N, 40°W [see *Lumpkin and Garzoli*, 2005, Figure 1].

[14] Below the pycnocline, at the SACW levels (~150–500 m), the NBC retroflects at 3°–6°N, 47°–50°W and feeds into the generally eastward North Equatorial Undercurrent (NEUC), which represents the southern limb of the tropical cyclonic gyre [*Cochrane et al.*, 1979; *Wilson et al.*, 1994; *Johns et al.*, 1998]. From the NBC retroflection site, the undercurrent departs southeastward, then (at 3°–4°N) turns eastward [see *Johns et al.*, 1998, Figure 18] and proceeds to the eastern equatorial basin, where the NEUC extension turns northeastward thus delivering SACW, also known as "13°C water" [*Tsuchiya*, 1986], to the eastern tropical North Atlantic [*Schmitz and McCartney*, 1993; A98].

[15] The Ioffe-2000 data confirm the cyclonic flow of the subsurface waters in the equatorial North Atlantic below the pycnocline. The NEUC/SACW equatorward pathway is seen from the abrupt eastward ascent of the isopycnals (26.6–27.0 kg m^{-3}) in the westernmost part of the section at 45°–46.5°W (~4°N). In the eastern basin, relatively weakly stratified SACW layer ($26.0 < \sigma_0 < 27.0$ kg m^{-3}) is observed east of 31°–32°W (north of ~6.5°N) between ~100 and 400 m. It should be noted that according to *Elmoussaoui et al.* [2005], the NEUC/SACW cyclonic flow occurs in the region above the isopycnal $\sigma_0 = 26.8$ kg m^{-3}, and below this density level, the Central Water has a North Atlantic origin.

[16] The poleward passages of the NEUC in the eastern basin are seen from eastward deepening of the isopycnals at 28°–31.5°W (below ~150 m) and 21.5°–24.5°W (below ~100 m). The steep isopycnal slopes at 30°–31.5°W (i.e., at the western margin of the weakly stratified SACW layer) suggest an intense jet-like northeastward current, similar to the one previously observed in the 7.5°N section at ~29°–31°W and farther north in the 11°N section at ~26°–29°W [see *Stramma et al.*, 2005b, Figures 11a and 13a]. The

second northeastward passage of the NEUC in the eastern basin (at 21.5°–24.5°W in the Ioffe-2000 section) was also detected at 7.5°N, ~21°–23°W [see *Stramma et al.*, 2005b, Figure 13a].

[17] Thus the upper ocean circulation across the Ioffe-2000 section is mostly dominated by the eastward near-surface NECC detected between 5.3°N and 7.8°N (~23°–38°W), most intense at ~5.5°–6°N, and by the subsurface NEUC, cyclonic flow of which is crossed by the section line at ~45°–46°W (4°N) above the Amazon Cone and east of ~31°W (north of 6.5°N) in the eastern equatorial basin. Schematic representation of the described circulation is proposed in Figure 3b.

4. Properties and Main Circulation Features of the Intermediate, Deep, and Bottom Waters

4.1. Intermediate Waters

[18] The intermediate waters are seen as a low-salinity and high-silicate anomaly that extends along the section (Figures 2b and 2d) at the depths of ~400–1200 m. The major sources of these waters are the northward flows of the Antarctic Intermediate Water (AAIW) and the Upper Circumpolar Water (UCPW), and it is considered that the traditional hydrographic tracers do not allow one to separate them from each other in the low latitudes [*Tsuchiya et al.*, 1994; A98]. In the potential temperature-salinity diagram based on the Ioffe-2000 data (Figure 4), UCPW is indeed indistinguishable from AAIW.

[19] One of the signatures of UCPW that allows identification of this water separately from AAIW is the vertical minimum of potential temperature [*Reid*, 1989]. The temperature minimum layer (~4.6°–4.8°C) is observed in the westernmost part of the section (west of ~38°W) at depths of ~900–1200 m (Figure 2a). It should be noted that in a number of studies [*Wüst*, 1935; *Tsuchiya et al.*, 1994; A98], this temperature minimum was interpreted as the lower boundary of AAIW and it was supposed to be a result of superposition of AAIW and the North Atlantic Deep Water.

[20] The other and the main characteristic of UCPW in the equatorial region is the intermediate maximum of silicate concentrations [*Oudot et al.*, 1998]. Along the entire Ioffe-2000 section, the silicate maximum (>28 μmol kg^{-1}, ~900–1000 m) is located deeper than the salinity minimum (~34.55–34.70, ~750 m) and lies near the isopycnal σ_0 = 27.40 kg m^{-3}, while the salinity minimum is located mostly above and near the isopycnal σ_0 = 27.30 kg m^{-3}. This silicate maximum (up to 31 μmol kg^{-1} in the western basin) can be recognized as a result of the northward spreading of UCPW in view of the fact that the silicate concentrations in the core of AAIW at its origin are about 30 μmol kg^{-1} [see *Tsuchiya et al.*, 1994; *Oudot et al.*, 1998]. The most evident confirmation of the UCPW presence north of the equator is seen from the potential temperature–silicate diagram, in which the data points from the western basin form a distinct θ-Si extremum at 4.7°–4.8°C, 30–31 μmol kg^{-1}, while in the θ-S plot the minimum salinity values are associated with temperatures noticeably higher than 4.8°C (see Figure 4).

[21] The main entrance of AAIW to the North Atlantic is contoured by the 34.6 isohaline in Figure 2b west of 36°W. The CITHER-1 hydrographic observations at 7.5°N did not detect the clear trace of boundary flow of AAIW along the American continental slope (A98), while the nutrient fields showed this flow [*Oudot et al.*, 1998, 1999]. Direct 10-month current measurements at 8°N [*Johns et al.*, 1990] also showed the AAIW boundary flow as well as its strong temporal variability, which caused its regular extinction and even southward reversion. The Ioffe-2000 section ends in immediate proximity to the upper part of the Brazilian slope but actually does not reach the latter. Nevertheless, the general northward pathways of AAIW are seen in Figure 2b away from the western edge of the section as detached patches of the lowest salinities (<34.55) at ~42°–44°W and 46°–47°W.

[22] A noticeable rise of the upper part of the AAIW layer (to depths of ~250 m) is seen from a domelike distribution of temperature and salinity between 42°W and 45°W, that points to the local extrusion of the warm component (SACW) of the thermohaline cell return limb by its cool one (AAIW). Taking into account the section orientation, a general eastward rise of isopycnals σ_0 = 27.20 and σ_0 = 27.30 kg m^{-3} along the section indicates the eastward cross-sectional flow of AAIW. For instance, the σ_0 = 27.30 kg m^{-3} isopycnal located at 800 m at the western boundary rises toward the continental slope of Guinea to depths of less than 750 m (Figure 3a). Two separate domains of low salinity (<34.65) observed in the eastern basin at 23°–30°W (Figure 2b) are likely produced by the zonal jets of AAIW, since these salinity minima are accompanied by the pronounced eastward ascent of the isopycnals. A zonal flow of AAIW in the northern equatorial Atlantic is also evident from the float observations, which showed an eastward cyclonic flow pattern at intermediate levels in this region [see *Fratantoni and Richardson*, 1999, Figure 1].

[23] The potential temperature pattern shows the major northward flow of UCPW west of ~38°W (Figure 2a) but there are no distinct signs of the concrete pathways within the temperature minimum layer. These pathways are seen from two offshore intermediate maxima of silicate (>30 μmol kg^{-1}, Figure 2d) located at 38°–42°W and 43°–47°W. Thus the Ioffe-2000 data show that the major outflows of the intermediate waters (both AAIW and UCPW) from the western equatorial basin to the tropical North Atlantic likely occurred in the interior ocean, but not along the Brazilian slope. A similar result for UCPW only was derived at 7.5°N from the CITHER-1 nutrient data [see *Oudot et al.*, 1998].

4.2. North Atlantic Deep Water

[24] The high-saline, oxygen-rich and nutrient-poor North Atlantic Deep Water (NADW) penetrates into the equatorial Atlantic at the depths down to >3500 m [*Wüst*, 1935] mainly as the Deep Western Boundary Current (DWBC) [*Fine and Molinari*, 1988] and further bifurcates into an eastward flow and another one continuing southward along the western boundary [e.g., *Molinari et al.*, 1992; *McCartney*, 1993]. The NADW is commonly divided into the three following components [*Wüst*, 1935]: the Upper NADW (UNADW) recognizable from the middepth salinity maximum, the Middle NADW (MNADW) and the Lower NADW (LNADW) distinguishable mostly by the oxygen maxima at 2000–2500 m and ~3700 m, respectively. Therefore the Ioffe-2000 salinity and silicate data provide a clear identification of UNADW only (this water is seen from the distinct

extrema both in the θ-S and θ-S i plots, Figure 4), while for an evident distinction of MNADW and LANDW oxygen data would be necessary.

[25] In the western basin, the southward boundary flow of UNADW is clearly visible from the high-salinity domain (>35.0) against the continental slope at the depths of 1400–1500 m. If a level of no motion is chosen at the UCPW–UNADW boundary (~1200 m), a northward recirculation of UNADW is seen from the reversal of the isopycnal slopes both sides of the MAR at 36°–40°W and 29°–32°W accompanied with the isolated salinity maximum (>34.98) and isothermal perturbations at ~31°–32°W. Recirculation of UNADW revealed in the western basin east of 40°W generally agrees with the UNADW circulation pattern inferred by *Friedrichs and Hall* [1993, Figure 10a], according to which a part of the UNADW southeastward boundary flow reverses between 5°N and the equator, crosses the Ioffe-2000 section latitude (~5°N) at ~40°W and proceeds northwestward.

[26] The sharp near-slope break of the isopycnals at ~1900–2600 m denotes the offshore southward flow of MNADW. The slopeward deepening of isopycnals shows the narrow (<100 km) northward recirculation of the DWBC at the MNADW depths. Below 2700 m, the eastward deepening of the isopycnals ($\sigma_2 \geq 37.04$ kg m^{-3}) confirms the general southward path of NADW along the American slope. The deep cyclonic cell in the Guiana basin [*McCartney*, 1993; *Friedrichs and Hall*, 1993; *Richardson and Schmitz*, 1993; A98] is indicated by the eastward ascent of the isopycnals near the western slope of the Ceara Rise and east of the Rise between ~42°W and 36°–37°W. This northward recirculation is most clearly seen below ~3000 m in the LNADW layer. At the $\sigma_4 \approx 45.90$ kg m^{-3} density level, recirculating LNADW joins the northward flow of the Antarctic Bottom Water (AABW).

[27] In the eastern basin, NADW is less saline and richer in silicate, as seen from the θ-S and θ-Si plots (Figure 4); the vertical and zonal structure of NADW east of the MAR is noticeably more homogeneous than in the western basin. The only distinguishable component of the NADW, the UNADW, is still visible here in the reduced form as a tongue of increased salinity (~34.95–34.98) and low silicate content (~19–23 μmol kg^{-1}). The hydrographic tracers show the dominance of LNADW in the near-bottom layer of the eastern basin west of the Sierra Leone Rise: the potential temperature (>1.8°C), salinity (~34.88) and density (~$45.88 < \sigma_4 < 45.89$ kg m^{-3}) in this layer are the same as above and near the lower boundary of LNADW ($\sigma_4 \approx 45.90$ kg m^{-3}) west of the MAR, see Figures 2a–2c and the θ-S plot in Figure 4. The eastward rise of the isopycnals $\sigma_2 = 37.02$ kg m^{-3} – $\sigma_4 = 45.86$ kg m^{-3} east of the Sierra Leone Rise indicates the northward cyclonic flow of NADW through the Kane Gap into the southeastern part of the Gambia Basin.

4.3. Antarctic Bottom Water

[28] In the equatorial Atlantic, a part of AABW flows northwestward to the Guiana Basin through the Equatorial Channel and the Ceara Abyssal Plain [*McCartney and Curry*, 1993], while a remainder penetrates into the eastern basin through the Romanche and Chain Fracture Zones [*Mercier and Speer*, 1998] where it moves further east into the Guinea and Angola Basins and to the north into the Sierra Leone Basin [*Mercier et al.*, 1994; A98].

[29] The northward flow of AABW is clearly seen west of the MAR in the near-bottom layer ($\sigma_4 > 45.90$ kg m^{-3}) of the Para Abyssal Plain as a domain countered by the 34.88 isohaline and 1.8°C isotherm. The minimum benthic values of temperature and salinity (0.962°C, 34.784) are found in the 40–42°W trough, into which AABW arrives moving directly along the Ceara Rise eastern slope, as was previously shown from the 4.5°N section of R/V *Meteor* 27 cruise [*Rhein et al.*, 1998]. The steep eastward rise of the isopycnals $\sigma_4 = 45.90$–45.94 kg m^{-3} at the same longitudes is another signature of the main path of AABW through the central western basin, but not along the western foot of the MAR where the isopycnal slopes are reversed, indicating the AABW southward recirculation.

[30] The strong mixing with LNADW in the equatorial fracture zones radically modifies all the properties of AABW as it penetrates into the eastern basin [*Mercier and Morin*, 1997]. Nevertheless, bottomward decrease of potential temperature and salinity to the values of about 1.8°C and 34.88 indicates the AABW presence in a residual form in the almost homogeneous near-bottom layer ($\sigma_4 > 45.88$ kg m^{-3}) east of ~28°W (north of 7°N). The lowest temperature and salinity values (1.810°C, 34.873) are found east of the Sierra Leone Rise that likely points to the possible weak exchange of AABW between the Sierra Leone Basin and the Gambia Abyssal Plain (fed by the Vema Fracture Zone [*McCartney et al.*, 1991]) through the Kane Gap. Distribution of all the properties show that this exchange is obviously negligible in comparison with the general northward flow of AABW observed in the section east of the Ceara Rise in the western basin [see also *Mantyla and Reid*, 1983; *McCartney et al.*, 1991; A98; *Oudot et al.*, 1998].

5. The 1993–2000 Temperature Changes in the Eastern Basin

[31] Comparison of the temperature data from transatlantic sections carried out along 8.25°N in 1957 (R/V *Crawford*) and along 7.5°N (WOCE A06 line) in 1993 (R/V *L'Atalante*) has shown the warming (~0.1°C–0.15°C) of the upper ~2800-m layer and less pronounced cooling (<0.03°C) at deeper levels (A98). In the central part of the eastern basin, the upper ~2800-m layer became warmer by up to ~0.05°C–0.15°C, while the deeper waters became colder by less than 0.05°C between the 1957 and 1993 observations (see A98). The qualitatively similar results for the eastern basin of the subtropical North Atlantic have been obtained at 24°N from the comparison of the 1957 and 1992 temperature data [see *Parrilla et al.*, 1994]. The revealed changes have been attributed to a deepening of the middepth isotherms, but not to a modification of the temperature–salinity correlation (A98).

[32] In order to evaluate possible 7-a changes in vertical distribution of temperature in the eastern basin between 1993 and 2000, the temperature differences were computed for the 22°–28°W parts of the CITHER-1 7.5°N and Ioffe-2000 sections. The 22°–28°W longitude range centered in the crossing point of these sections at 25°W was chosen so that the meridional distance between the ends of the section

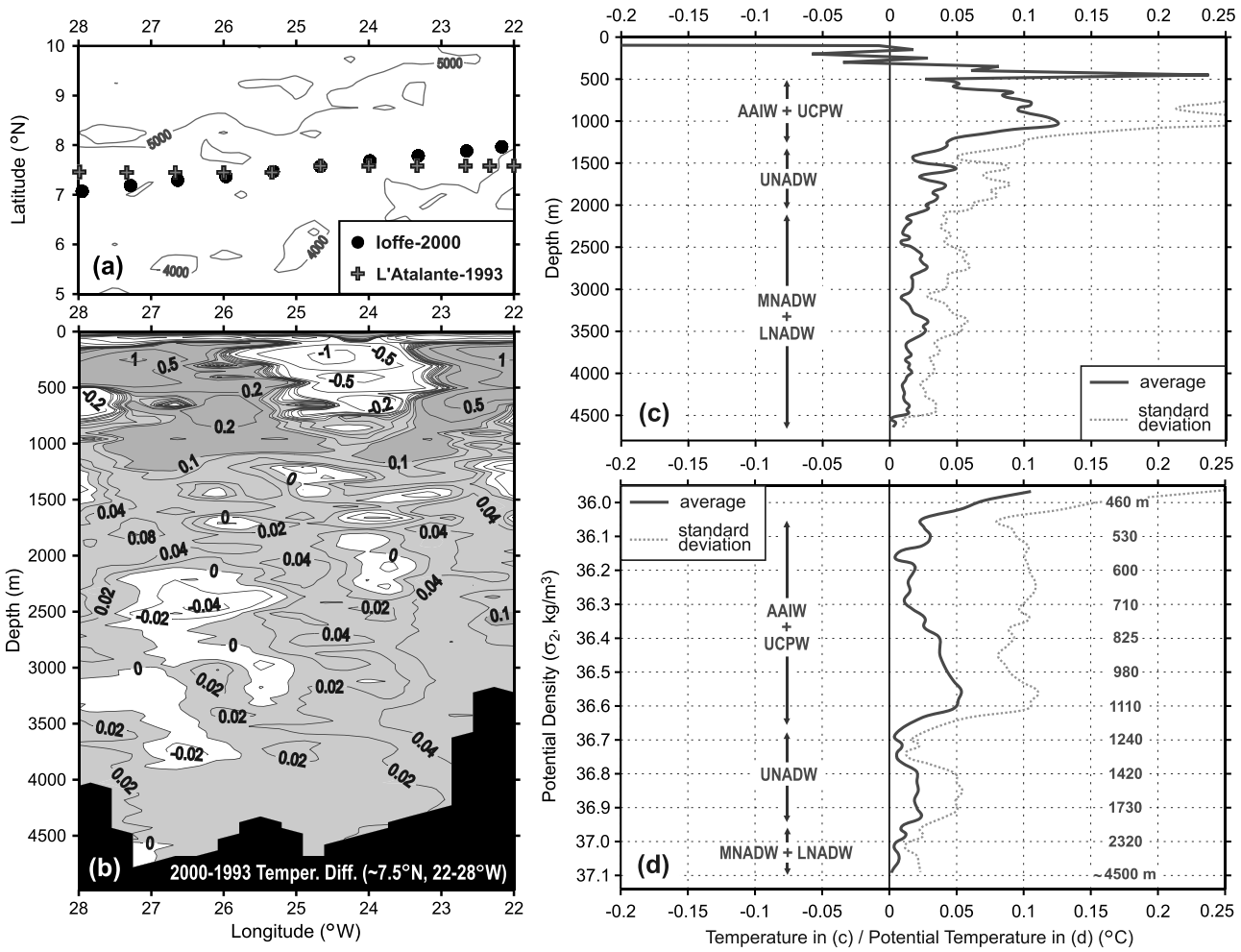

Figure 5. Temperature differences between the 22°–28°W parts of the sections carried out on board the R/V *Akademic Ioffe* in 2000 and the R/V *L'Atalante* (WOCE A06 line, 7.5°N) in 1993. (a) Locations of the stations used for the comparison. (b) Vertical distribution of the 2000–1993 temperature differences; positive values indicating warming are shaded. (c) Profile of zonally averaged temperature differences shown in Figure 5b. (d) Profile of zonally averaged 2000–1993 potential temperature differences on isopycnals (σ_2, kg m^{-3}) at the intermediate and deeper levels calculated for the same longitude range (22°–28°W); approximate depths of the isopycnals are marked. In Figures 2c and 2d, the approximate depth and density intervals corresponding to the water mass layers are shown with arrows; see text for water mass abbreviations. Locations of the Ioffe-2000 section and the WOCE A06 line are given in Figure 1.

parts (~50 km) was not critical to the comparison and, on the other hand, a substantial number of stations was involved.

[33] Locations of the stations used for computation of the 2000–1993 temperature differences (11 stations from the 1993 cruise, 10 stations from the 2000 one) are shown in Figure 5a. The pattern of differences and their zonally averaged profile are displayed in Figures 5b and 5c, respectively. Salinity differences between the 1993 and 2000 sections were also calculated for the 22°–28°W longitude range; these differences are not discussed (and not shown) herein as they are of the order of 10^{-3} and thus are comparable to the accuracy of salinity measurements.

[34] The profile of averaged temperature differences (Figure 5c) shows that the water column below ~500 m in the central eastern basin of the equatorial Atlantic at ~7.5°N, 22°–28°W became warmer between the 1993 and 2000 observations. Temperature changes in the upper 500-m layer are not considered, since the sections were carried out in different seasons. It should be noted that on the background of prevailing warming, which is also clearly seen from the vertical distribution of differences, there are several domains of negative temperature anomalies as well as those of extremely high positive values (see Figure 5b). This "mosaic" distribution reflects, most likely, variations in the regional circulation pattern, which could cause the local changes in the temperature distribution and thus produce interrelated (and mutually compensated) local maxima and minima of temperature differences. Lateral averaging reduces this effect and therefore seems to be effective in quantification of actual temperature changes (resulted from a modification of the water mass properties and/or changes

in the layer thicknesses), but not just in representation of comparison results.

[35] The most pronounced average warming is revealed at the intermediate (AAIW–UCPW) levels. Temperature in the intermediate layer (~500–1250 m) increased by 0.05°C–0.12°C (Figure 5c), in average for the layer, by 0.082°C.

[36] The warming at deeper (NADW) levels is of a more limited intensity not exceeding 0.05°C. The UNADW (~1250–2000 m) layer became warmer by 0.02°C–0.05°C; below 2000 m, at the MNADW–LNADW levels, temperature increased by 0.01°C–0.03°C (Figure 5c). The vertically averaged temperature increase is twice as high in the UNADW layer (0.032°C) than in that of MNADW–LNADW (0.016°C). Overall, the NADW bulk (1250–4500 m) became warmer by 0.020°C.

[37] A slight warming signal of less than 0.01°C is detected in the benthic layer (below 4500 m) east of 27°W (Figures 5b and 5c), where the weak influence of AABW was observed (see section 4.3). The vertically averaged warming in this layer is just of 0.003°C, which is comparable to the accuracy of temperature measurements.

[38] In order to evaluate a contribution of the water mass temperature changes to the revealed net warming, the 2000–1993 potential temperature differences on isopycnals (σ_2) were calculated for the same (22°–28°W) longitude range. Profile of zonally averaged differences on isopycnals is given in Figure 5d. Figure 5d shows that the isopycnal differences (reflecting changes in the water mass temperatures [see *Arbic and Owens*, 2001]) at intermediate and deeper levels are generally less than the changes at corresponding depths (Figure 5c), but also are positive. The intermediate waters ($36.05 < \sigma_2 < 36.65$ kg m^{-3}) became warmer on isopycnals in average by 0.032°C, that is about 60% less than the average warming (+0.082°C) at constant depth levels in the corresponding depth range (500–1250 m). The vertically averaged isopycnal warming (+0.009°C) in the NADW layer ($\sigma_2 \geq 36.65$ kg m^{-3}) is 55% less than the temperature increase (+0.020°C) detected in the NADW depth range (>1250 m). The near-bottom temperature changes on isopycnals are the same (+0.003°C) as the zonally averaged temperature differences at the near-bottom depths. Thus the contribution of the water mass temperature increase to the net warming is from about 40 (for the intermediate waters) to 45% (for NADW).

[39] The distinct warming of the intermediate and upper deep waters, in general, corresponds to the warming of the upper ~2800-m layer in the eastern basin previously revealed at this latitude from the 1957–1993 comparison. The average 1993–2000 warming of the 500–2800 m water column (0.046°C) extrapolated over 36 a would be 0.23°C, which is at least two times higher than temperature increase of ~0.1°C that occurred over 36 a from 1957 to 1993 (see A98).

[40] Comparison of the 1957 and 1993 data has shown the cooling of less than 0.05°C below ~2800 m in the eastern basin [see A98], while from 1993 to 2000, the 2800–4500 m layer became warmer, in average, by 0.014°C, which is equivalent to the temperature increase of 0.07°C per 36 a. Thus the rate of the 1993–2000 warming of deep waters below 2800 m exceeds the rate of previously revealed cooling.

[41] In general, the results obtained at ~7.5°N from the 1957–1993 and 1993–2000 comparisons together with those obtained at 24°N point to the warming of the upper ocean at low latitudes of the North Atlantic since the late 1950s, which may have intensified in the eastern basin at 7.5°N in the 1990s. At the same time, the results of comparison of only three (1957, 1993 and 2000) snapshots are certainly not enough to reliably evaluate a magnitude of the apparent long-term trend. The shorter-scale variability in the region could be substantial during the 1957–2000 time period (and hence crucial for reliability of such evaluation), as likely follows from the 1957–1993–2000 temperature changes at deeper levels. These changes point to either the change of cooling trend below ~2800 m to a warming tendency, or just to the significance of temperature fluctuations in the region on timescales of a decade or less.

6. Summary

[42] For the first time since 1993 the transocean quasi-zonal hydrographic section in the equatorial North Atlantic was occupied in July 2000 on board the Russian R/V *Akademik Ioffe*. In this paper, the water mass structure and the main circulation features in this key transit region for the global circulation are discussed using the temperature, salinity, potential density and silicate distributions along the section. Comparison of the newly acquired temperature data with those obtained by the French R/V *L'Atalante* at 7.5°N in 1993 is carried out for the interior eastern basin in order to reveal the 7-a changes at intermediate and deeper levels.

[43] Since the Ioffe-2000 cruise was performed in summer and the cruise track is not strictly zonal, the distinct signatures of the season-dependent eastward NECC are observed. The cross-sectional flow of the NECC above 100–150 m between 5.3°N and 7.8°N (~23°–38°W) is evident from the potential density distribution; this flow is most intense at its southern border (south of 6°N). At the subsurface levels, below the NECC, the cross-sectional circulation is dominated by the cyclonic flow of the NEUC, which is known to carry SACW from the NBC retroflection through the equatorial region to the eastern tropical basin. Clear signatures of the NEUC are found in the westernmost part of the section at ~4°N, 45°–46.5°W, where the isopycnal slopes indicate the equatorward direction of the undercurrent, and in the eastern basin, where the northward pathways of the NEUC are observed at 28°–31.5°W and 21.5°–24.5°W.

[44] The main meridional flows of intermediate and deep waters are detected in the westernmost part of the section. The boundary flows are revealed only at the UNADW and LNADW levels, while the northward pathways of AAIW and UCPW and the southward one of MNADW are offshore.

[45] In the western basin, UCPW is clearly distinguishable from AAIW by both the potential temperature minimum and maximum of silicate content observed at a larger depth (~900–1000 m) than the depth of the salinity minimum (~750 m). The eastward zonal flow of AAIW across the section is indicated by the general section-wide ascent of isopycnals (within the AAIW stratum) between the continental slopes of Brazil and Guinea.

[46] Recirculation of all the components of NADW is observed both in the western and eastern basins. The northward reverse flow is most distinct in the MNADW layer against the Brazilian continental slope and in the LNADW layer between the Ceara Rise and the MAR and east of the Sierra Leone Rise in the eastern basin. A northwestward recirculation is also detected in the UNADW layer east of 40°W in western basin and over the eastern slope of the MAR at 29°–32°W.

[47] The major arrival of AABW to the North Atlantic occurs in the central western basin closer to the Ceara Rise than to the MAR, along the western foot of which AABW recirculates southward. East of ~28°W, the bottom water properties are similar to those observed in the western basin at the LNADW–AABW boundary that points to the presence of AABW strongly diluted with LNADW in the eastern basin north of 7°N.

[48] Comparison of the 2000 temperature data with the data obtained at the WOCE A06 line (7.5°N) in 1993 showed that the entire water column below 500 m in the central part of the eastern basin in 2000 was warmer than in 1993. This probable warming is most pronounced at the intermediate (AAIW–UCPW) levels (+0.08°C), less intense in the NADW bulk (+0.02°C), and almost unexpressed immediately near the bottom. It is shown that the apparent net warming is to a large extent (roughly by 40–45%) caused by the increase of the water mass temperatures.

[49] The 1993–2000 temperature increase at intermediate and upper deep levels in the central eastern basin together with previously reported results of the 1957–1993 comparison at ~7.5–8°N allow one to assume a long-term warming above 2500–3000 m in the interior eastern equatorial North Atlantic during the second half of the 20th century.

[50] **Acknowledgments.** We thank captains, crews, and chief scientists of the cruises *Akademik Ioffe* 8 and *L'Atalante* CITHER-1. The work of all who contributed to processing of the data is also highly appreciated. Our special thanks to Michel Arhan for useful suggestions. The anonymous reviewers are gratefully acknowledged for their constructive comments that helped to improve the manuscript. This study was supported by the Russian Ministry of Education and Science under the contract 02.515.11.5032.

References

Andrie, C., J. F. Ternon, M. J. Messias, and L. Memery (1998), Chlorofluoromethane distributions in the equatorial Atlantic during January–March 1993, *Deep Sea Res., Part I*, *45*, 903–930.

Arbic, B. K., and W. B. Owens (2001), Climatic warming of Atlantic Intermediate Waters, *J. Clim.*, *14*, 4091–4108.

Arhan, M., H. Mercier, B. Bourles, and Y. Gouriou (1998), Hydrographic sections across the Atlantic at 7°30N and 4°30N, *Deep Sea Res., Part I*, *45*, 829–872.

Blanke, B., M. Arhan, A. Lazar, and G. Prévost (2002), A Lagrangian numerical investigation of the origins and fates of the salinity maximum water in the Atlantic, *J. Geophys. Res.*, *107*(C10), 3163, doi:10.1029/2002JC001318.

Broecker, W. S. (1985), The great ocean conveyor, *Oceanography*, *4*, 79–89.

Cochrane, J. D., F. J. Kelly, and C. R. Olling (1979), Subthermocline countercurrents in the western equatorial Atlantic Ocean, *J. Phys. Oceanogr.*, *9*, 724–738.

Dickson, R. R., and J. Brown (1994), The production of North Atlantic Deep Water: Sources, rates, and pathways, *J. Geophys. Res.*, *99*(C6), 12,319–12,342.

Elmoussaoui, A., M. Arhan, and A.-M. Tréguier (2005), Model-inferred upper ocean circulation in the eastern tropics of the North Atlantic, *Deep Sea Res., Part I*, *52*, 1093–1120, doi:10.1016/j.dsr.2005.01.010.

Fine, R. A., and R. L. Molinari (1988), A continuous deep western boundary current between Abaco (26.5°N) and Barbados (13°N), *Deep Sea Res.*, *35*, 1441–1450.

Fratantoni, D., and P. L. Richardson (1999), SOFAR float observations of an intermediate-depth Eastern Boundary Current and mesoscale variability in the eastern tropical Atlantic Ocean, *J. Phys. Oceanogr.*, *29*, 1265–1278.

Friedrichs, M. A., and M. M. Hall (1993), Deep circulation in the tropical North Atlantic, *J. Mar. Res.*, *51*, 697–736.

Fuglister, F. L. (1960), Atlantic Ocean atlas of temperature and salinity-profiles and data from the International Geophysical Year of 1957–1958, *Woods Hole Oceanogr. Inst. Atlas Ser. 1*, 209 pp., Woods Hole Oceanogr. Inst., Woods Hole, Mass.

Gordon, A. L. (1986), Interocean exchange of thermocline water, *J. Geophys. Res.*, *91*(C4), 5037–5046.

Johns, W. E., T. N. Lee, F. A. Schott, R. J. Zantopp, and R. H. Evans (1990), The North Brazil current retroflection: Seasonal structure and eddy variability, *J. Geophys. Res.*, *95*(C12), 22,103–22,120.

Johns, W. E., T. N. Lee, R. C. Beardsley, J. Candela, R. Limeburner, and B. Castro (1998), Annual cycle and variability of the North Brazil Current, *J. Phys. Oceanogr.*, *28*, 103–128.

Lumpkin, R., and S. L. Garzoli (2005), Near-surface circulation in the tropical Atlantic Ocean, *Deep Sea Res., Part I*, *52*, 495–518.

Macdonald, A. M. (1998), The global ocean circulation: A hydrographic estimate and regional analysis, *Prog. Oceanogr.*, *41*, 281–382.

Mantyla, A. W., and J. L. Reid (1983), Abyssal characteristics of the world ocean waters, *Deep Sea Res., Part A*, *8*, 805–833.

McCartney, M. S. (1993), Crossing of the equator by the Deep Western Boundary Current in the western Atlantic Ocean, *J. Phys. Oceanogr.*, *23*, 1953–1974.

McCartney, M. S., and R. A. Curry (1993), Transequatorial flow of Antarctic Bottom Water in the western Atlantic Ocean: Abyssal geostrophy at the equator, *J. Phys. Oceanogr.*, *23*, 1264–1276.

McCartney, M. S., S. L. Bennett, and M. E. Woodgate-Jones (1991), Eastward flow through the Mid-Atlantic Ridge at 11°N and its influence on the abyss of the eastern basin, *J. Phys. Oceanogr.*, *21*, 1089–1121.

Mercier, H., and P. Morin (1997), Hydrography of the Romanche and Chain fracture zones, *J. Geophys. Res.*, *102*(C5), 10,343–10,389.

Mercier, H., and K. G. Speer (1998), Transport of bottom water in the Romanche Fracture Zone and Chain Fracture Zone, *J. Phys. Oceanogr.*, *28*, 779–790.

Mercier, H., K. G. Speer, and J. Honorez (1994), Flow pathways of bottom water through the Romanche and Chain fracture zones, *Deep Sea Res., Part I*, *41*, 1457–1477.

Molinari, R. L., R. A. Fine, and E. Johns (1992), The deep western boundary current in the tropical North Atlantic Ocean, *Deep Sea Res.*, *39*, 1967–1984.

Mullin, J. B., and J. P. Riley (1955), The spectrophotometric determination of silicate-silicon in natural waters with special reference to sea water, *Anal. Chim. Acta*, *12*, 162–170.

Oudot, C., P. Morin, F. Baurand, M. Wafar, and P. Le Corre (1998), Northern and southern water masses in the equatorial Atlantic: Distribution of nutrients on the WOCE A6 and A7 Lines, *Deep Sea Res., Part I*, *45*, 873–902.

Oudot, C., J. F. Ternon, C. Andrie, E. S. Braga, and P. Morin (1999), On the crossing of the equator by intermediate water masses in the western Atlantic Ocean: Identification and pathways of Antarctic Intermediate Water and Upper Circumpolar Water, *J. Geophys. Res.*, *104*(C9), 20,911–20,926.

Parrilla, G. A., A. Lavin, H. Bryden, M. Garcia, and R. Millard (1994), Rising temperatures in the subtropical north Atlantic over the past 35 years, *Nature*, *369*, 48–51.

Reid, J. L. (1989), On the total geostrophic circulation of the South Atlantic Ocean: Flow patterns, tracers and transports, *Prog. Oceanogr.*, *23*, 149–244.

Rhein, M., L. Stramma, and G. Krahmann (1998), The spreading of Antarctic bottom water in the tropical Atlantic, *Deep Sea Res., Part I*, *45*, 507–527.

Richardson, P. L., and T. K. McKee (1984), Average seasonal variation of the Atlantic Equatorial Currents from historical ship drifts, *J. Phys. Oceanogr.*, *14*, 1226–1238.

Richardson, P. L., and W. J. Schmitz Jr. (1993), Deep cross-equatorial flow in the Atlantic measured with SOFAR floats, *J. Geophys. Res.*, *98*(C5), 8371–8387.

Rintoul, S. R. (1991), South Atlantic interbasin exchange, *J. Geophys. Res.*, *96*(C2), 2675–2692.

Schmitz, W. J. (1995), On the interbasin-scale thermohaline circulation, *Rev. Geophys.*, *33*, 151–173.

Schmitz, W. J., and M. S. McCartney (1993), On the North Atlantic circulation, *Rev. Geophys.*, *31*, 29–49.

Schott, F., J. Fischer, J. Reppin, and U. Send (1993), On mean and seasonal currents and transports at the western boundary of the equatorial Atlantic, *J. Geophys. Res.*, *98*(C8), 14,353–14,368.

Stramma, L., M. Rhein, P. Brandt, M. Dengler, C. Böning, and M. Walter (2005a), Upper ocean circulation in the western tropical Atlantic in boreal fall 2000, *Deep Sea Res., Part I*, *52*, 221–240.

Stramma, L., S. Hüttl, and J. Schafstall (2005b), Water masses and currents in the upper tropical northeast Atlantic off northwest Africa, *J. Geophys. Res.*, *110*, C12006, doi:10.1029/2005JC002939.

Tsuchiya, M. (1986), Thermostads and circulation in the upper layer of the Atlantic Ocean, *Prog. Oceanogr.*, *16*, 235–267.

Tsuchiya, M., L. D. Talley, and M. S. McCartney (1994), Water-mass distributions in the western South Atlantic; a section from South Georgia Island (54S) northward across the equator, *J. Mar. Res.*, *52*, 55–81.

Wilson, W. D., E. Johns, and R. L. Molinari (1994), Upper layer circulation in the western tropical North Atlantic Ocean during August 1989, *J. Geophys. Res.*, *99*(C11), 22,513–22,523.

Wüst, G. (1935), Schichtung und Zirkulation des Atlantischen Ozeans. Das Bodenwasser und die Stratosphäre, in *Wissenschaft Ergebnisse der Deutschen Atlantischen Expedition auf dem Forschungs- und Vermessungsschiff "Meteor" 1925–1927*, vol. 6, edited by W. Krauß and A. Defant, pp. 1–288, de Gruyter, Berlin.

A. Demidov, Department of Oceanology, Moscow State University, GSP-2, Leninskie Gory, 119992 Moscow, Russia.

A. Sarafanov and A. Sokov, P. P. Shirshov Institute of Oceanology, 36 Nakhimovskiy Prospect, 117997 Moscow, Russia. (sarafanov@mail.ru; sokov@ocean.ru)